A NUMERICAL STUDY OF CAVITATION INFLUENCE ON DIESEL JET ATOMISATION

J.B. Moreau*, O. Simonin°, C. Habchi*

* IFP, 1 et 4 avenue de Bois-Préau, 92852 Rueil-Malmaison Cedex – France
° Institut de Mécanique des Fluides de Toulouse, Allée du Professeur Camille Soula, 31400 Toulouse – France
Corresponding author: chawki.habchi@ifp.fr

ABSTRACT

This work consists in studying the effects of Diesel injector internal flow on liquid jet atomisation phenomenon downstream of the nozzle exit. A 3D numerical multiphase code (referred to as CAVIF) has been developed to calculate both cavitation and jet atomisation processes for high pressure conditions. This code is based on a homogeneous description similar to Dumont et al. model [1]: it solves a compressible and viscous Navier-Stokes system for a single fluid with a mixture (i.e. liquid and vapour fuel + air) density ρ_m and a pressure P calculated using a newly developed bidimensional barotropic equation of state of the form $P = f(\rho_m, Y_f)$ where Y_f is the mass fraction of fuel. This equation of state relies on the perfect gas law for pure air and an integrated two-phase (liquid fuel and its vapour) sound speed equation from Wallis [2]. In addition to mass and momentum balance equations, a transport equation for the mass fraction of fuel Y_f has been used as a fuel tracer. Results of a 2D single hole injector simulation show the effect of cavitation on jet atomisation: a cavitating bubble leaving the injector nozzle induces a liquid-air interface perturbation which leads to a strong jet instability. These results seem to be qualitatively similar to several experimental data [3-6].

INTRODUCTION

Diesel spray atomisation is greatly influenced by cavitation occurring inside injectors (Soteriou et al. [7]). Because of high speed flow inside the injector nozzle, small orifices, short injection duration and very high pressure, experimental investigations in real-size nozzles are difficult and numerical simulation is a promising approach for a better understanding of the flow topology (Habchi et al. [8]).

In order to simulate properly atomisation, cavitating flows have to be considered in the numerical model. This model has to take into account multiphase flows representing the fuel (i.e. liquid + cavitation bubbles) coming from the injector and the gas (i.e. air) of the combustion chamber.

A 3D code called CAVIF has been developed by Dumont et al. [1]. It is based on a homogeneous model, where the multi-phase mixture is treated as a pseudo-fluid m that obeys the usual equations of single-phase flow. Suitable average properties are determined (velocity, density, viscosity), varying between properties of each pure phase. The difficult part of developing such models is deriving a meaningful and stable equation for pressure. The new version of CAVIF is now able to deal with the air (i.e. gas g) of the combustion chamber. The new equation of state (EOS) has been interpolated between the equation of Wallis [2] and the ideal gas equation. This relation gives the pressure as a function of ρ_m (mixture density) and Y_f (fuel mass fraction in the whole mixture m composed of fuel f and gas g).

2D simulations of typical injector geometry have been carried out. The effect of cavitation bubbles moving out of the injector on spray atomisation is highlighted and discussed, before drawing conclusions.

THE HOMOGENEOUS MODEL

The CAVIF code solves a compressible and viscous Navier-Stokes system, which consists in a continuity equation:

$$\frac{\partial \rho_m}{\partial t} + \frac{\partial(\rho_m u_j)}{\partial x_j} = 0 \tag{1}$$

and a momentum balance equation:

$$\frac{\partial(\rho_m u_i)}{\partial t} + \frac{\partial(\rho_m u_i u_j)}{\partial x_j} = -\frac{\partial P}{\partial x_i} + \frac{\partial \tau_{ij}}{\partial x_j} \tag{2}$$

where u_i represents the mixture velocity components (drift velocity between phases is neglected as we use a homogeneous approach with only one velocity for the mixture) and τ_{ij} is the viscous stress tensor defined as follows:

$$\tau_{ij} = \mu_m \left(\frac{\partial u_i}{\partial x_j} + \frac{\partial u_j}{\partial x_i} \right) - \frac{2}{3} \mu_m \frac{\partial u_i}{\partial x_i} \delta_{ij} \tag{3}$$

Surface tension and gravity are negligible compared to cavitation effects. As the EOS follows the rule $P = f(\rho_m, Y_f)$ we need a transport equation for the mass fraction of fuel Y_f, which acts as a fuel tracer:

$$\frac{\partial(\rho_m Y_f)}{\partial t} + \frac{\partial(\rho_m Y_f u_j)}{\partial x_j} = 0 \tag{4}$$

Thus the mixture density can be written:

$$\frac{1}{\rho_m} = \frac{Y_f}{\rho_f} + \frac{(1 - Y_f)}{\rho_g} \tag{5}$$

where ρ_f is the density of the fuel mixture (liquid + vapour) and ρ_g is the gas density. Therefore the fuel volume fraction is defined by the relation:

$$\alpha_f = \frac{\rho_m - \rho_g}{\rho_f - \rho_g} \tag{6}$$

The mixture viscosity μ_m is calculated as an arithmetical mean between the fuel and the gas viscosity like Kubota [9]:

$$\mu_m = \alpha_f \mu_f + (1 - \alpha_f)\mu_g \tag{7}$$

Inside the injector the volume fraction of vapour in fuel (or void fraction) is defined by:

$$\alpha_v = \frac{\rho_f - \rho_l}{\rho_v - \rho_l} \tag{8}$$

where ρ_v and ρ_l are respectively the pure fuel vapour and liquid density. The fuel viscosity μ_f is also calculated as:

$$\mu_f = \alpha_v \mu_v + (1 - \alpha_v)\mu_l \tag{9}$$

THE EQUATION OF STATE (EOS)

The main difficulty of a homogeneous model is the closure of the Navier-Stokes system. The EOS used in CAVIF is based on Wallis equation for the fuel and on the ideal gas equation for the air.

EOS governing the two-phase fuel mixture ($f = l + v$)

Following Avva *et al.* [10], the starting point is a conservation of energy statement:

$$\frac{\partial(\rho_f h)}{\partial t} + \frac{\partial(\rho_f h u_j)}{\partial x_j} = \frac{\partial P}{\partial t} + P\frac{\partial u_j}{\partial x_j} + \frac{\partial}{\partial x_j}\left(k\frac{\partial T}{\partial x_i}\right) + \frac{\partial u_i}{\partial x_j}\tau_{ij} \tag{10}$$

where h is the fuel mixture enthalpy and k the thermal conductivity. In Diesel injection conditions, thermal conduction and viscous work can be neglected from the energy equation. The remaining terms describe reversible work and suggest that in place of the energy equation one may use an isentropic model equation as Schmidt [11]:

$$dP = c_f^2 d\rho_f \tag{11}$$

where the acoustic speed c_f of the two-phase flow ($l + v$) is given by Wallis [2] (see Figure 1):

$$\frac{1}{c_f^2} = \left[\alpha_v \rho_v + (1 - \alpha_v)\rho_l\right]\left[\frac{\alpha_v}{\rho_v c_v^2} + \frac{(1 - \alpha_v)}{\rho_l c_l^2}\right] \tag{12}$$

Figure 1 shows that the sound speed decreases dramatically when the fluid is not composed of a single phase, due to the multiple reflections of the waves between the mixture interfaces. Considering the acoustic speed as constant in pure vapour and pure liquid, we can calculate the continuous EOS governing the fuel mixture by integrating Eq. (11) between the saturation pressure P_l^{sat} at the liquid-vapour interface and the indicated pressure P (see Figure 2):

$$\begin{cases} P = \rho_f c_v^2 & \text{if } \rho_f \leq \rho_v \\ P = P_l^{sat} + \frac{\rho_v c_v^2 \rho_l c_l^2 (\rho_v - \rho_l)}{\rho_v^2 c_v^2 - \rho_l^2 c_l^2}\ln\left[\frac{\rho_v c_v^2\left(\rho_l + \alpha_v(\rho_v - \rho_l)\right)}{\rho_l\left(\rho_v c_v^2 - \alpha_v(\rho_v c_v^2 - \rho_l c_l^2)\right)}\right] & \text{if } \rho_v < \rho_f < \rho_l \\ P = P_l^{sat} + (\rho_f - \rho_l)c_l^2 & \text{if } \rho_f \geq \rho_l \end{cases} \tag{13}$$

In this model vapour induced by cavitation is not included in the gas phase and is considered as a phase in full measure.

EOS governing the gas (g)

Inside the combustion chamber the gas (third phase) is governed by the ideal gas equation:

$$P = \rho_g \frac{R}{W_g} T_g \tag{14}$$

where W_g is the gas molecular weight, T_g the gas temperature and R is the universal gas constant. In this model we assume that the gas temperature is constant.

Three-phase mixture EOS building ($m = l + v + g$)

The aim is to develop a relation of the form $P = f(\rho_m, Y_f)$ where ρ_m comes from the continuity equation Eq. (1) and Y_f from the transport equation Eq. (4).
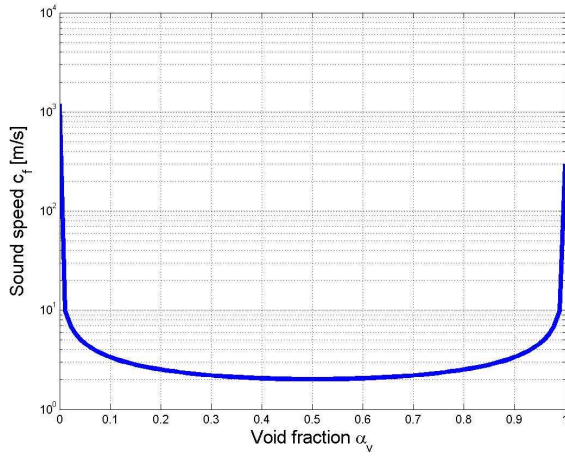
Figure 1: *Sound speed c_f versus void fraction α_v (Wallis [2])*
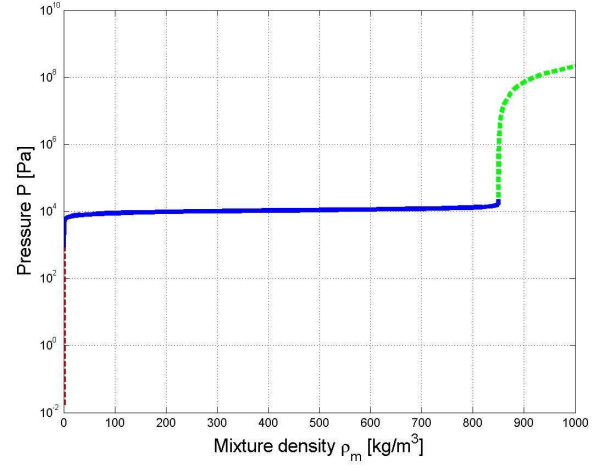

Figure 2: *Two-phase EOS governing the fuel $(l + v)$ with its 3 characteristic parts*

The main assumption for this EOS determination is that we consider a thermodynamic equilibrium between the fuel f and the gas g at fuel-gas interfaces, so that the pressure P in f is the same as in g. This leads to an instantaneous collapse of cavitation bubbles just after leaving the injector hole. As a matter of fact, collapse is induced by a pressure increase in the cavitating region.

The only way to link P, ρ_m and Y_f is to calculate $\rho_m = f(P, Y_f)$. Giving a couple (ρ_f, Y_f) in the range of values that can be reached during computation, the pressure P corresponding to ρ_f is calculated using Eq. (13). As we assume an equilibrium at fuel f and gas g interfaces, Eq. (14) gives ρ_g and the determination of ρ_m is made possible through Eq. (5) giving Y_f. By scanning the range of ρ_f and Y_f we are able to build a grid surface: $\rho_m = f(\rho_f, Y_f)$, that is to say $\rho_m = f(P, Y_f)$ because setting ρ_f is equivalent to setting P.

The grid surface on Figure 3 stands for the whole mixture EOS. This continuous surface is composed of three parts that correspond to the three different fuel compositions of Wallis EOS. The first part concerns a mixture that contains the phases v and g (Figure 4). The second one is used when there is $(l + v + g)$ in the computation cell (Figure 5). Finally the third one deals with $(l + g)$ mixture (Figure 6). The first two parts of the EOS concern so low pressures that we cannot see them properly on Figure 3.

Then we will have to use an interpolation method to determine the relation $P = f(\rho_m, Y_f)$ between the tabulated grid values. Obviously the interpolation accuracy depends on the given (P, Y_f) grid refinement: it must be chosen carefully, especially in the $(l + v + g)$ domain (Figure 5) because of the very steep slope of the surface.

Three-phase EOS surface interpolation

During CAVIF simulations ρ_m and Y_f are known at any time in each computation cell thanks to Eq. (1) and Eq. (4). The relation $P = f(\rho_m, Y_f)$ can be determined by interpolation between the tabulated grid values. Due to the distorted shape of the surface, a global interpolation of the whole surface is difficult. We prefer a piecewise interpolation on the same grid as the one used for the EOS building. A least-square method allows a first order interpolation:

$$P = A + B\rho_m + CY_f + D\rho_m Y_f \tag{15}$$

For each couple of values (ρ_m, Y_f) (i.e. for each subsurface of the EOS grid) we calculate the coefficients A, B, C and D using the 4 vertices of the subsurface. Those coefficients are tabulated in CAVIF code and an algorithm scans the data base to find the values corresponding to the considered subsurface at each time step and for each computation cell.
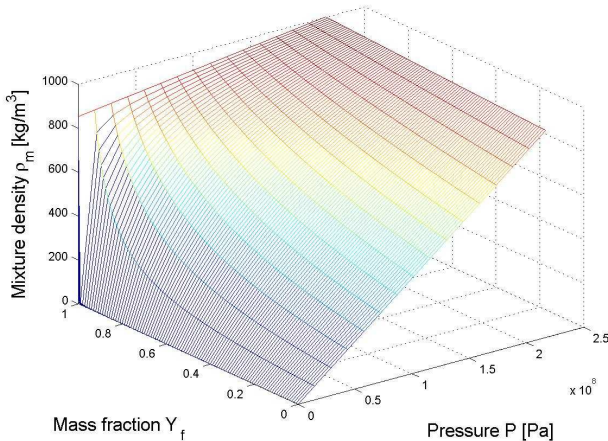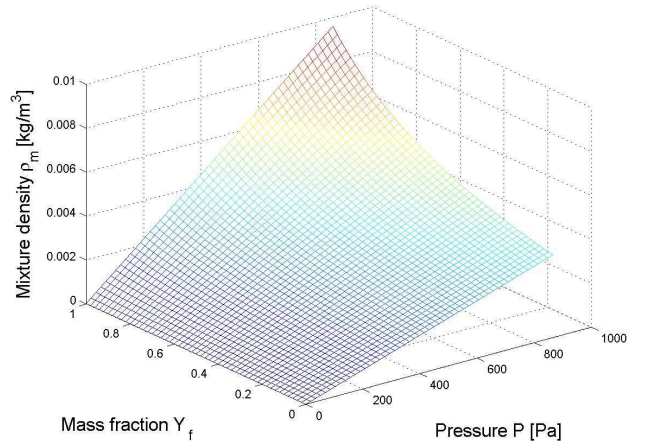

Figure 3: *The whole three-phase EOS surface*

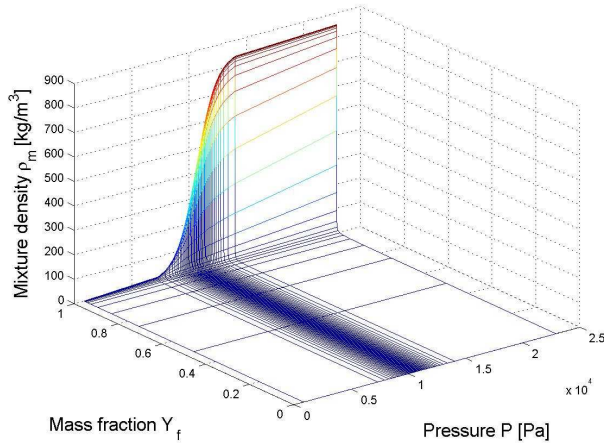Figure 4: *Lower part of the three phase EOS $(v + g)$*

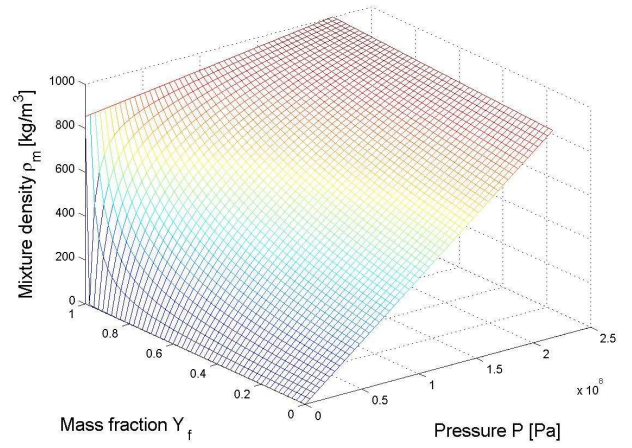Figure 5: *Three-phase EOS governing the mixture when (l + v + g) coexist*

Figure 6: *Upper part of the three-phase EOS (l + g)*

DIESEL INJECTOR CONFIGURATION TEST

In order to study the effect of cavitation on Diesel jet atomisation using the model described previously, a bi-dimensional planar test case was achieved. In this test, liquid fuel ($\rho_l = 850$ kg/m^3, $\mu_l = 7.98 \ 10^{-3}$ kg/m s, $\rho_g/\rho_l = 0.051$) is injected at 100 MPa in a chamber initially full of air at 5 MPa. The computational domain represents a typical injector geometry: the nozzle diameter is 200 µm (considering a symmetry axis on the right) and its length is 1 mm. The mesh consists in 100*400 cells for the whole cavitating computational domain ($dx = 5$ µm and $dz = 20$ µm in the nozzle). For simulations without cavitation, a 100*300-cell mesh is used because we do not need to simulate the flow upstream of the hole; however the lower part of the mesh is strictly the same as in cavitating case.

Figure 7 and 8 show the evolution of mixture density with and without cavitation. One can notice that the beginning of the two simulations is very similar, but as soon as cavitation appears ($t = 4.2$ µs), at the sharp inlet edge of the hole, jet destabilisation is affected. A *vena contracta* is created inside the hole, inducing a flow acceleration as it is explained by Dumont *et al.* [12]. The leading part of the liquid jet is immediately perturbed and the spray angle is increased (Eifler [3]). Between $t = 4.2$ µs and $t = 7.1$ µs, cavitation grows in the nozzle and reaches the hole exit. Previous computations without gas chamber leaded to a supercavitation regime [1, 8]. In our computations cavitation is very transient and a supercavitating regime is never reached. As cavitation moves out of the injector the collapse induced by the pressure difference between gas and vapour leads to a jet pinching ($t = 8.5$ µs). This phenomenon influences the jet downstream and upstream, inducing a destabilisation of the jet ($t = 9.9$ µs), as it was noticed by Miranda *et al.* [4] and Eifler [3]. The liquid in the chamber is fractionated by subsequent cavitation bubble exit. This seems to have an important effect on jet atomisation. This jet fractionating behaviour is in qualitatively good agreement with Verhoeven *et al.* [5] visualisations using a Mie scattering technique and with Bruneaux [6] PLIF experiments in similar operating conditions.

Figure 8 shows that without cavitation the bulk properties of the liquid, namely viscosity and density, result in a stable jet. To make sure that the low density observed in Figure 7 inside the nozzle is fuel vapour (and not gas), Figure 9 and 10 show the fuel mass fraction value is 1 in the region where vapour (i.e. cavitation) appears.
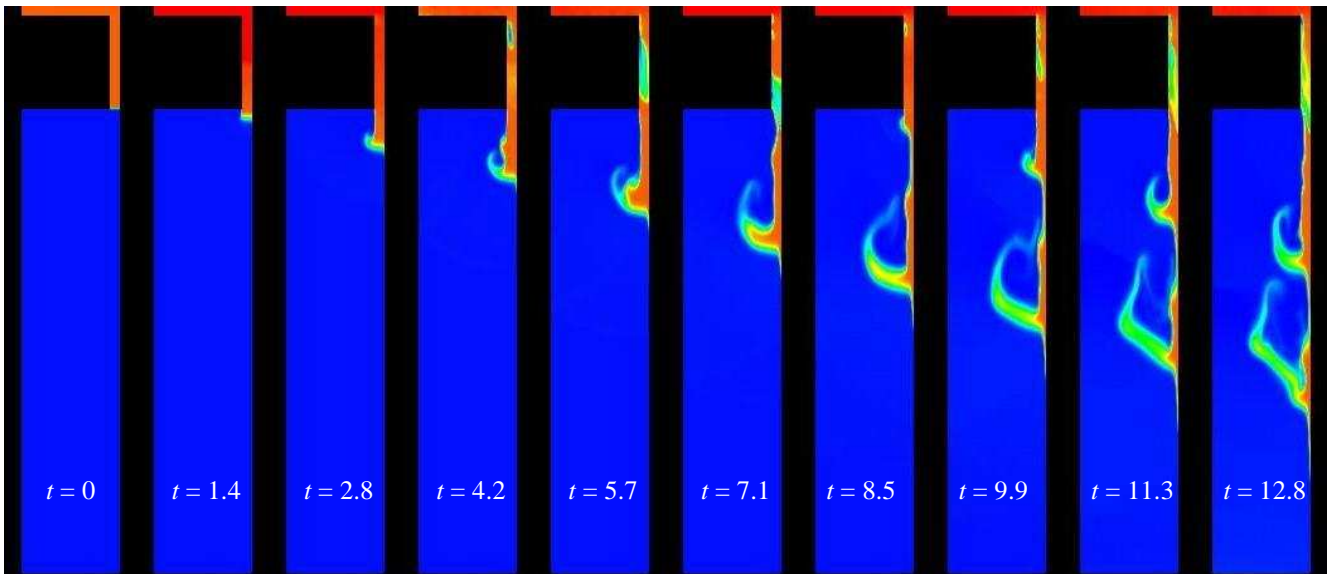

Figure 7: *Mixture density ρ_m field computational results for fuel injection into gas in Diesel conditions ($P_{inj} = 100$ MPa, $P_{ch} = 5$ MPa) with cavitation (time t in µs, see colour scale in Figure 11)*
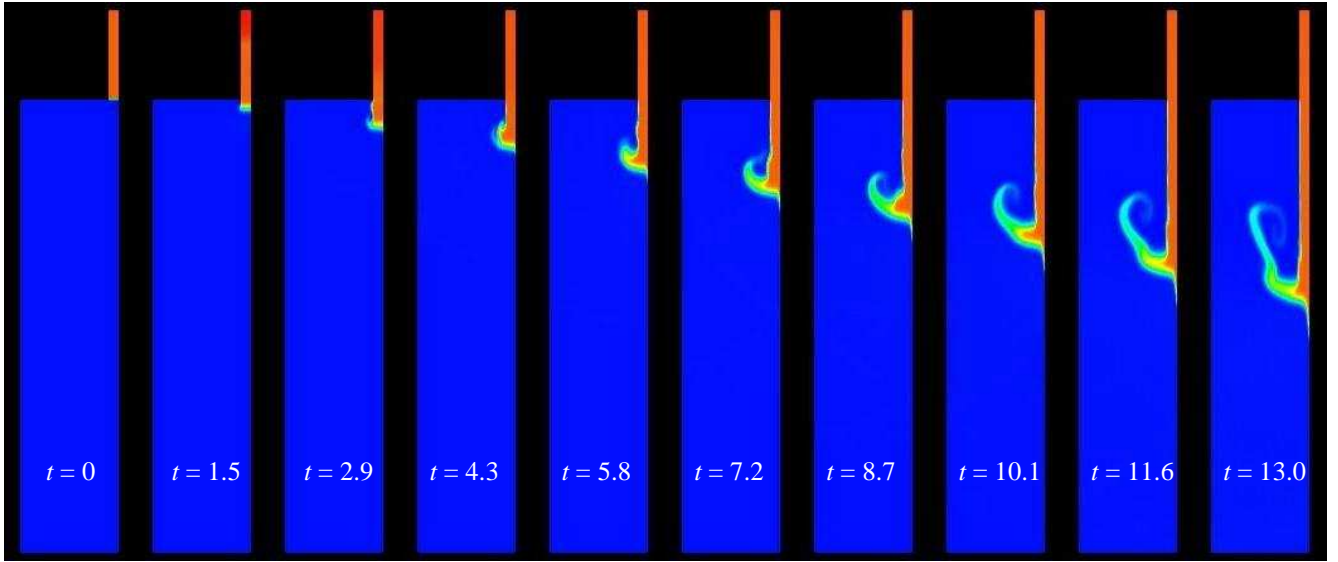
Figure 8: *Mixture density ρ_m field computational results for fuel injection into gas in Diesel conditions (P_{inj} = 100 MPa, P_{ch} = 5 MPa) without cavitation (time t in µs, see colour scale in Figure 11)*

Let us now focus our attention on the velocity profiles at the nozzle outlet (Figure 11). We observe that cavitation leaving the nozzle induces velocity profile variations, showing once more the unsteadiness of this phenomenon. The outlet maximal velocity oscillates between 250 and 525 m/s. On the one hand, when a vapour bubble reaches the outlet near the exit edge (t = 7.1 µs), the pressure gradient between gas and vapour leads to a re-entrant air flow. On the other hand, when a cavitating bubble leaves the nozzle inside the liquid flow (t = 7.8 µs), a pinching of the jet occurs because of the cavitation collapse. Consequently primary atomisation seems to be the result of two combined effects:

(i) gas-fuel interface strong perturbation due to vapour bubbles leaving the orifice near the exit edge hole.

(ii) pinching of the liquid column due to vapour bubble collapse near the orifice axis.

CONCLUSIONS

In this paper a 3D, viscous, unsteady numerical code called CAVIF has been presented. This code allows to simulate jet destabilisation and primary atomisation resulting from cavitation produced inside Diesel injectors.

A homogeneous approach is used to model three-phase flows. An equation of state which represents both fuel (either liquid or vapour) and gas has been developed. It is based on the assumption that the pressure in the fuel and in the gas are the same at any time at fuel-gas interfaces.

Computations of a liquid fuel injection into a 2D air chamber has been presented to study the effect of cavitation on the atomisation process. When cavitation appears inside the nozzle, the flow is accelerated and the leading part of the jet is immediately perturbed. The flow is very transient and a supercavitation regime is never reached, unlike previous computations without gas chamber. Cavitation leaving the injector hole immediately collapse, inducing a jet pinching and, as a consequence, a jet destabilisation that is qualitatively similar to experimental visualisations.

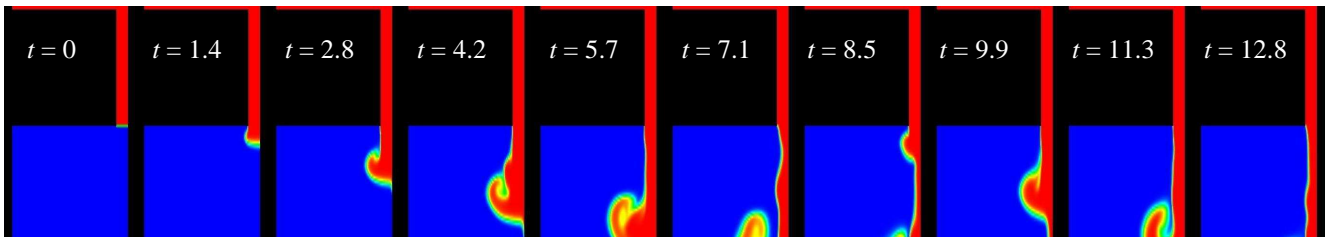These tests also show the model robustness and ability using the new EOS in CAVIF.

Figure 9: *Fuel mass fraction Y_f field for cavitating case: the colour scale is blue (Y_f = 0) to red (Y_f = 1) and time t is in µs*
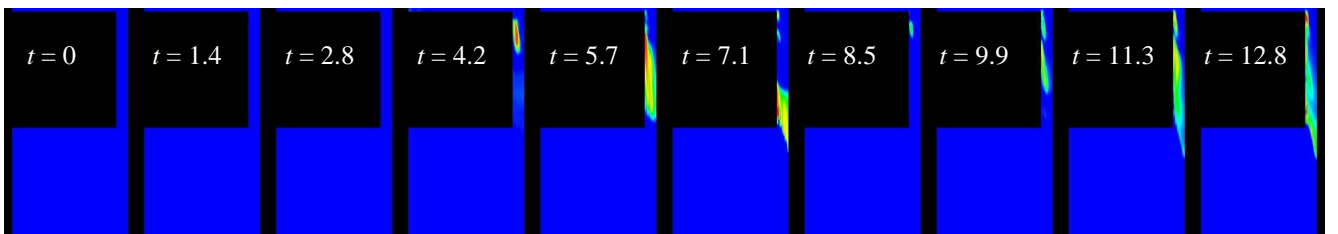

Figure 10: *Vapour (or void) fraction inside fuel α_v field for cavitating case: the colour scale is blue (α_v = 0) to red (α_v = 1) and time t is in µs*
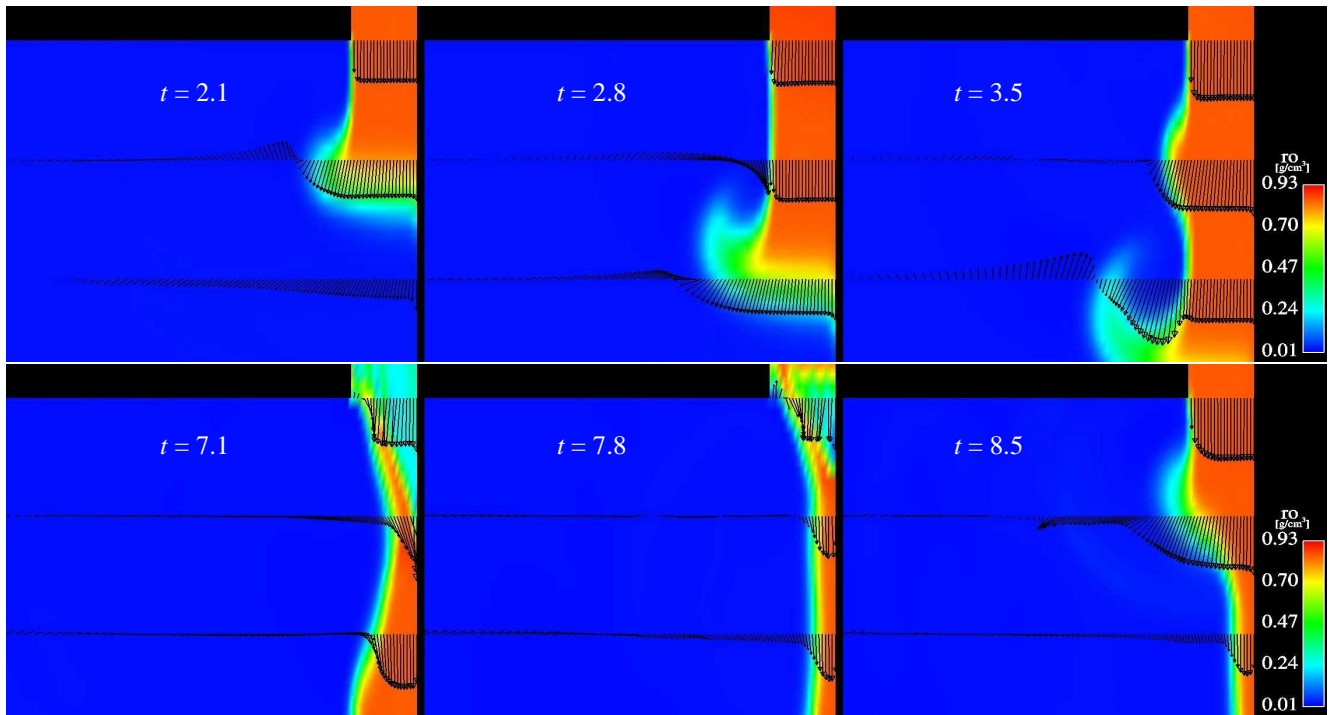
Figure 11: *Zoom of cavitating case results including three velocity profiles at 0, 1 and 2 diameters from the orifice exit (time t in µs); ρ_m field in the background*

NOMENCLATURE

Latin symbols
c sound speed (m/s)
dx cell size along radial direction (m)
dz cell size along flow axis (m)
h specific enthalpy (J/kg)
k thermal conductivity (W/m K)
P pressure (Pa)
R universal gas constant (J/K)
t time (s)
T temperature (K)
u velocity (m/s)

W molecular weight (kg)
x spatial direction (m)
Y mass fraction (dimensionless)

Greek symbols
α volume fraction (dimensionless)
δ Kronecker symbol (dimensionless)
μ dynamic viscosity (kg/m s)
ρ density (kg/m^3)
τ viscous stress tensor (kg/m s²)

Subscript
f fuel (either liquid or vapour)
g gas phase (i.e. air)
l fuel liquid phase
m fuel and gas mixture
v fuel vapour phase

Superscript
sat at saturation

REFERENCES

1. N. Dumont, O. Simonin and C. Habchi, Numerical Simulation of Cavitating Flows in Diesel Injectors by a HEM Approach, *Proc. Fourth International Symposium of Cavitation*, Pasadena, USA, 2001.
2. G.B. Wallis, *One-dimensional Two-phase Flow*, McGraw-Hill, 1969.
3. W. Eifler, Untersuchungen zur Struktur des Instationären Dieselöleinspritzstrahles im Düsennahbereich mit der Methode der Hochfrequenz-Kinematografie, Ph.D. thesis, Universität Kaiserslautern, Germany, 1990.
4. R. Miranda, H. Chaves and F. Obermeier, Imaging of Cavitation, Hollow Jets and Jet Branching at Low Lift in a Real Size VCO Nozzle, *Proc. ILASS-Europe 2002*, Zaragoza, Spain, 2002.
5. D. Verhoeven, J.L. Vanhemelryck and T. Baritaud, Macroscopic and Ignition Characteristics of High-pressure Sprays of Single-component Fuels, *SAE technical paper 981069*, 1998.
6. G. Bruneaux, Optical Diagnostics of High Pressure Common Rail Diesel Sprays: Liquid and Vapor Phase Visualization, *Proc. Fourth International Conference on Multiphase Flow*, New Orleans, USA, 2001.
7. C. Soteriou, R. Andrews and M. Smith, Direct Injection Diesel Sprays and the Effect of Cavitation and Hydraulic Flip on Atomization, *SAE technical paper 950080*, 1995.
8. C. Habchi, N. Dumont and O. Simonin, CAVIF: a 3D Code for the Modeling of Cavitating Flows in Diesel Injectors, *Proc. ICLASS 2003*, Sorrento, Italy, 2003.
9. A. Kubota, H. Kato and H. Yamaguchi, A New Modeling of Cavitated Flow: a Numerical Study of Unsteady Cavitation on a Hydrofoil Section, *J. Fluid Mech.*, vol. 240, pp. 59-69, 1992.
10. R.K. Avva, A. Singhal and D.H. Gibson, An Enthalpy Based Model of Cavitation, *Proc. ASME FED*, vol. 226, 1995.
11. D.P. Schmidt, Cavitation in Diesel Fuel Injector Nozzles, Ph.D. thesis, University of Wisconsin, Madison, USA, 1997.
12. N. Dumont, O. Simonin and C. Habchi, Cavitating Flow in Diesel Injectors and Atomization: a Bibliographical Review, *Proc. ICLASS 2000*, Pasadena, USA, 2000.